Topological Interface Engineering and Defect Crossing in Ultracold Atomic Gases

Magnus O. Borgh* and Janne Ruostekoski†

School of Mathematics, University of Southampton, SO17 1BJ, Southampton, United Kingdom

(Received 23 February 2012; published 3 July 2012)

We propose an experimentally feasible scheme for topological interface engineering and show how it can be used for studies of dynamics of topologically nontrivial interfaces and perforation of defects and textures across such interfaces. The method makes use of the internal spin structure of the atoms together with locally applied control of interaction strengths to create many-particle states with highly complex topological properties. In particular, we consider a constructed coherent interface between topologically distinct phases of spinor Bose-Einstein condensates.

DOI: 10.1103/PhysRevLett.109.015302 PACS numbers: 67.85.Fg, 03.75.Lm, 03.75.Mn, 11.27.+d

At the interface of two topologically distinct phases of a macroscopically coherent quantum system, the symmetry properties of the ground-state wave function change. Topological defects (e.g., vortices) cannot in general penetrate the interface unchanged. The boundary therefore has the property that defects must either terminate on the interface (typically as a point defect or monopole) or connect nontrivially to another object on the opposite side of the boundary.

Interfaces between topologically distinct regions play an important role, e.g., in exotic superconductivity [1], superfluid liquid ^{3}He A-B mixtures [2–4], and in early-universe cosmology. It has been proposed that a series of symmetry breakings lead to formation of domain walls and cosmic strings, which terminate on the boundaries between regions of different vacuum states [5,6]. Highly complex interface physics also arises from collisions between branes [7] in string-theory brane-inflation [8] scenarios. Superfluids have been discussed as candidates for experimentally accessible systems where analogues of cosmic topological defects may be studied [3,9]. For example, colliding liquid ^{3}He A-B interfaces have been proposed as analogues of string-theory branes [10].

Here we show how atomic-physics laboratory techniques can be employed for engineering topologically nontrivial, coherent interface boundaries between spatially separated different ground-state manifolds that simultaneously exhibit different broken symmetries. We demonstrate nontrivial penetration of singular defects across a constructed stable interface between ferromagnetic (FM) and polar phases of a spin-1 Bose-Einstein condensate (BEC). We identify the basic defect solutions crossing the interface and minimize their energies in order to characterize the defect core structures. We find examples of intriguing core deformations where a singular vortex terminates as an arch defect on the interface with the topological charge of a monopole, and where a coreless, nonsingular vortex connects to a pair of singular half-quantum vortices.

Our example demonstrates how the ultracold atom interface physics provides a novel medium for studies of stability properties of field-theoretical solitons [11–14]. The spin-1 BEC also already provides a possible system for dynamical investigation of phase transitions and defect production, e.g., of brane annihilation models. Moreover, the proposed method for interface engineering can exhibit especially rich phenomenology in spin-2 and spin-3 BECs and in strongly correlated optical lattice systems.

Atomic-physics technology provides tools for accurate detection methods for ultracold-atom systems on length and time scales that are difficult to achieve in laboratory systems of more traditional quantum fluids and solids. Advanced measurement techniques combined with the high degree of control over experimental parameters make them suitable for quantum simulators of physical phenomena that are too complex even for numerical studies. This has attracted considerable interest, in particular in optical lattice systems, which can emulate strongly correlated condensed-matter models. The experimental development for using ultracold atoms as a laboratory testing ground for complex physical phenomena has been accelerated, e.g., by the observations of the Mott-insulator states of atoms [15–17], by the study of nonequilibrium defect formation in phase transitions in the Kibble-Zurek mechanism for both scalar [18] and spin-1 BECs [19], and in the preparation of artificial gauge-field potentials for multilevel atoms [20].

Spinor BECs are condensates in which the spin degree of freedom is not frozen by magnetic trapping [21]. They provide ideal models and emulators of complex broken symmetries due to their rich phenomenology of different phases [22–28] that support exotic defects and textures [29–32]. Spinor BECs have attracted recent experimental attention, e.g., in the studies of formation of spin textures [33,34] and in controlled preparation [35,36] and nonequilibrium formation [19] of vortices.

Here we will concentrate on a spin-1 BEC whose macroscopic wave function $\Psi(\mathbf{r})$ may be written in terms of the local density $n(\mathbf{r})$ and a normalized spinor $\zeta(\mathbf{r})$ as

$$\Psi(\mathbf{r}) = \sqrt{n(\mathbf{r})}\zeta(\mathbf{r}) = \sqrt{n(\mathbf{r})}\begin{pmatrix}\zeta_+(\mathbf{r})\\ \zeta_0(\mathbf{r})\\ \zeta_-(\mathbf{r})\end{pmatrix}, \qquad \zeta^\dagger\zeta = 1. \quad (1)$$

In the Gross-Pitaevskii mean-field description, the Hamiltonian density of the spin-1 BEC reads

$$\mathcal{H} = \frac{\hbar^2}{2m}|\nabla\Psi|^2 + V(\mathbf{r})n + \frac{c_0}{2}n^2 + \frac{c_2}{2}n^2|\langle\hat{\mathbf{F}}\rangle|^2 + g_1 n\langle\mathbf{B}\cdot\hat{\mathbf{F}}\rangle + g_2 n\langle(\mathbf{B}\cdot\hat{\mathbf{F}})^2\rangle. \quad (2)$$

$\langle\hat{\mathbf{F}}\rangle = \zeta_\alpha^\dagger\hat{\mathbf{F}}_{\alpha\beta}\zeta_\beta$ is the expectation value of the spin operator $\hat{\mathbf{F}}$, defined as a vector of spin-1 Pauli matrices. A weak external magnetic field leads to linear and quadratic Zeeman shifts described by the last two terms. The two interaction strengths are $c_0 = 4\pi\hbar^2(2a_2 + a_0)/3m$ and $c_2 = 4\pi\hbar^2(a_2 - a_0)/3m$, respectively, where m is the atomic mass and a_0 and a_2 are the s-wave scattering lengths corresponding to the two different values of the relative angular momentum of the colliding atom pair.

The sign of c_2 determines which phase is energetically favored by the interaction alone. For $c_2 < 0$, as with ^{87}Rb, minimization of the interaction energy favors the FM phase with the maximum spin magnitude $|\langle\hat{\mathbf{F}}\rangle| = 1$ in which case the broken symmetry of the ground-state manifold is defined by the rotations of the spin vector. The FM phase supports two topologically distinct classes of line defects [22,23]. The nontrivial vortices in each class are singly quantized singular line defects and nonsingular coreless vortices, respectively [37], both of which have been observed [19,33,35,36].

If instead $c_2 > 0$, as with ^{23}Na, the interaction energy favors the polar phase, minimizing the spin magnitude $|\langle\hat{\mathbf{F}}\rangle| = 0$. The broken symmetry of the ground-state manifold is described by the unoriented nematic axis $\hat{\mathbf{d}}$ ($\hat{\mathbf{d}} = -\hat{\mathbf{d}}$) and the condensate phase ϕ. The polar phase therefore exhibits nematic order, analogously to liquid crystals and the superfluid liquid ^{3}He-A phase, and so supports both integer and half-quantum vortices.

Scattering lengths in ultracold-atom systems are routinely manipulated using magnetic Feshbach resonances. However, this is not possible in a spinor BEC since the required strong magnetic field would freeze out the condensate spin degree of freedom. It is possible to manipulate scattering lengths also through optical [38] or microwave-induced Feshbach resonances [39] in which case the fields can be kept sufficiently weak in order not to destroy the spinor nature of the BEC. The Feshbach resonance changes the scattering length by coupling the entrance channel to a virtually populated bound state [39]. In particular, it is possible to tune the ratio a_0/a_2 between the two scattering lengths.

We suggest constructing an interface between topologically distinct manifolds by spatially nonuniform engineering of the scattering lengths. In a spin-1 BEC this may be experimentally realized to prepare an interface between coexisting FM and polar phases. Using an optical Feshbach resonance, the spatial pattern corresponding to a sharp interface can be imposed using a holographic mask. The spin-dependent interaction strength c_2 is proportional to the difference between a_2 and a_0. Thus for small $|c_2|$, as is the case with both ^{87}Rb and ^{23}Na, only a small relative shift of a_0 versus a_2 is necessary to prepare the interface, and therefore the inelastic losses associated with optical Feshbach resonances [38] can be kept small.

A microwave field cannot similarly be focused. However, using an optically induced level shift to tune the microwave transition off-resonant where no adjustment of the scattering length is desired, interactions may be manipulated in spatially well-defined regions to prepare a sharp interface boundary without the losses associated with the optical Feshbach resonance.

In order to demonstrate the nontrivial nature of defect penetration across an interface between topologically distinct manifolds, we consider a harmonically trapped spin-1 BEC, where c_2 abruptly changes sign at the center of the trap at $z = 0$. We have $c_2 > 0$ for $z > 0$, corresponding to the polar phase, and for $z < 0$, the BEC is in the FM phase with $c_2 < 0$.

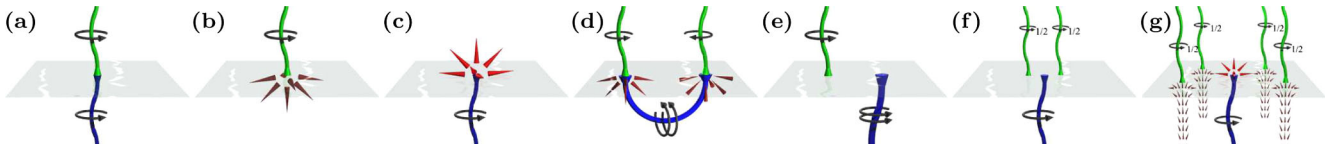

FIG. 1 (color online). Schematic illustrations of possible vortex connections. The polar phase is above the interface and the FM phase is below. (a) A singly quantized vortex in both phases. (b) A singly quantized vortex in the polar phase can connect to a Dirac monopole. The Dirac monopole can be continuously transformed into a coreless vortex. (c) A singly quantized spin vortex terminates as a polar monopole. (d) A dipole can be constructed by joining the Dirac strings of a Dirac monopole and an antimonopole [40]. Placed on the interface, the dipole connects to two singly quantized vortices on the polar side. (e) A singly quantized vortex in the polar phase connecting to a doubly quantized vortex on the FM side may be cut in half at the interface, and the resulting vortices in the two regions may be moved apart if an additional dark-soliton plane is introduced in ζ_0. More complicated vortex states may form as the splitting of a singly quantized polar vortex into two half-quantum vortices (f), or by nucleation of half-quantum vortices that connect to coreless vortices that may exist together with monopoles (g).

We first construct spinor solutions that approximate physical wave functions simultaneously in the two different manifolds and quickly relax to vortices connecting across the interface or terminating at the interface. Some illustrative examples of topologically allowed states are shown in Fig. 1. The simplest connection can be identified by considering a singly quantized vortex in both phases. Although such a vortex represents a very different topology in the two phases, it can be formed in both cases, e.g., by a 2π winding of the condensate phase ϕ around the z axis. The two vortex solutions can be joined by changing the sign of either ζ_+ or ζ_-. By appropriate choice of parameters, doing so causes the spinor wave function to adjust between the two manifolds by forcing $|\langle\hat{\mathbf{F}}\rangle|$ to switch from 0 to 1 [Fig. 1(a)] or else leads to a state which immediately relaxes to the desired configuration. Physically, such a sign change in one of the two spinor components can be obtained by introducing a dark-soliton plane (phase kink) in that component at $z = 0$, in which case the π-phase shift across the soliton is associated with a vanishing density at the soliton core. As the density of the other components at the soliton core does not vanish, the BEC wave function continuously connects the two manifolds. The interface acquires a width determined by the spin healing length $\xi_F = (8\pi|c_2|n)^{-1/2}$, the length scale over which $|\langle\hat{\mathbf{F}}\rangle|$ heals when locally perturbed.

A singular vortex with unit winding in the polar phase can also be written as a 2π spin rotation about the z axis together with a 2π rotation of the condensate phase ϕ. If we continue this solution to the FM side, by changing the sign of ζ_-, we identify the resulting structure as an approximation of a coreless vortex [22], in which the spin profile quickly acquires a fountain-like texture. Hence we have constructed a solution where a polar, singly quantized vortex connects to a FM coreless vortex [Fig. 1]. We parametrize the spinor as

$$\zeta^{1\leftrightarrow\mathrm{cl}} = \frac{1}{\sqrt{2}}\begin{pmatrix} -\sin\beta \\ \sqrt{2}e^{i\varphi}\cos\beta \\ \pm e^{2i\varphi}\sin\beta \end{pmatrix}, \tag{3}$$

where φ is the azimuthal coordinate, and $\beta = 3\pi/4$ gives an exact switch from polar to FM, with the negative sign in ζ_- used in the FM region.

If the coreless vortex in Eq. (3) is continuously deformed into a doubly quantized, singular vortex along the positive z axis terminating at the origin, the resulting spin texture on the FM side forms a radial hedgehog, $\langle\hat{\mathbf{F}}\rangle = \hat{\mathbf{r}}$. This structure can be identified as the analogue of the Dirac monopole in quantum field theory, with the singular vortex line representing the Dirac string [40] [Fig. 1(b)]. The deformation is possible due to topological equivalence between the doubly quantized vortex and the vortex-free state.

A singular spin vortex in the FM phase can be made to terminate on a polar monopole [Fig. 1(c)] as follows: The polar monopole is formed by two overlapping vortex lines of opposite circulation in $\zeta_\pm$ perpendicular to a soliton plane in ζ_0. The nematic axis then exhibits the radial hedgehog [29,30] $\hat{\mathbf{d}} = \hat{\mathbf{r}}$, which is the analogue of the t'Hooft-Polyakov monopole. Inserting a phase kink in ζ_+ at the interface results in a structure on the FM side where $\langle\hat{\mathbf{F}}\rangle$ points radially away from the z axis, which we identify as the spin vortex,

$$\zeta^{\mathrm{sv}\leftrightarrow\mathrm{pm}} = \frac{1}{\sqrt{2}}\begin{pmatrix} \mp e^{-i\varphi}\sin\theta \\ \sqrt{2}\cos\theta \\ e^{i\varphi}\sin\theta \end{pmatrix},$$

where θ and φ denote the spherical angles, and the positive sign is used in the FM part.

So far we have analyzed the topological existence of defects perforating the FM-polar interface. In order to determine their energetic stability and the core structure, we numerically minimize the energy of the constructed defect in a rotating frame $F = E - \Omega\langle\hat{L}_z\rangle$ by evolving the corresponding coupled spin-1 Gross-Pitaevskii equations in imaginary time. Here Ω denotes the frequency of rotation that is assumed to be around the z axis, $\langle\hat{L}_z\rangle$ is the z component of the angular momentum and $E = \int d^3r\mathcal{H}(\mathbf{r})$. We assume a slightly cigar-shaped trap $\omega_x = \omega_y = 2\omega_z \equiv \omega$ [41].

Minimizing the energy of $\zeta^{1\leftrightarrow\mathrm{cl}}$ results in the core deformation shown in Fig. 2. The state exhibits the coreless vortex on the FM side of the interface [Fig. 2(a)]. The frequency of rotation determines the direction of the spin vector at the edge of the cloud. The core of the singly

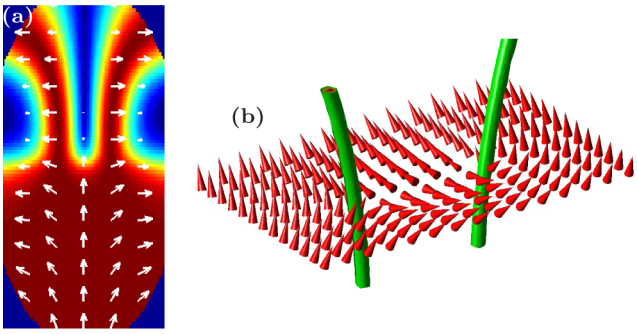

FIG. 2 (color online). Core structure after minimizing the energy of Eq. (3), corresponding to Fig. 1(b). (a) The magnitude of the spin [$|\langle\hat{\mathbf{F}}\rangle| = 1$ is dark red (dark gray) with long arrows]. The polar vortex has split into two half-quantum vortices with FM cores with nonvanishing densities. White arrows show the spin vector and indicate the coreless vortex in the FM part. Here $c_0 = 2.0 \times 10^4\hbar\omega l^3$, $|c_2| = 2.5 \times 10^2\hbar\omega l^3$, $\Omega = 0.12\omega$, and $B = 0$, where $l = (\hbar/m\omega)^{1/2}$ is the oscillator length (for ^{87}Rb with $\omega = 2\pi \times 10$ Hz this would correspond to 10^6 atoms). (b) The nematic axis $\hat{\mathbf{d}}$ (unoriented but shown as cones to emphasize winding) displays the characteristic π winding as each half-quantum vortex is encircled. The two cores are joined by a disclination plane indicating the turn of $\hat{\mathbf{d}}$ by π. ($|c_2| = 1.0 \times 10^4\hbar\omega l^3$, $\Omega = 0.19\omega$.)

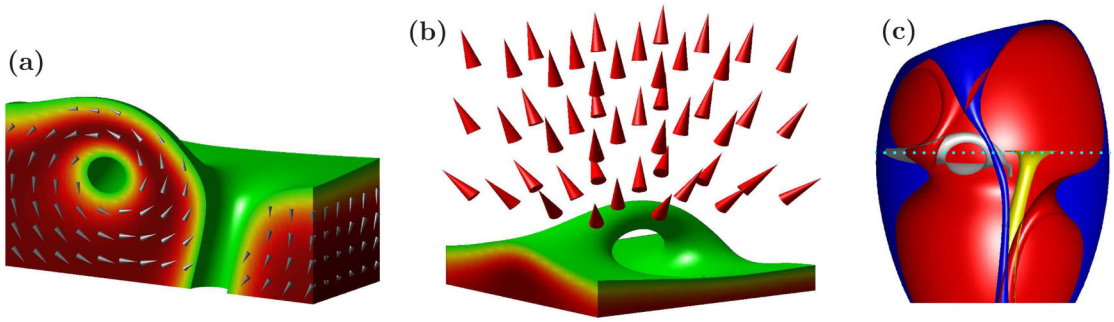

FIG. 3 (color online). Alice arch. When a singly quantized spin vortex terminates on a polar monopole, the point defect deforms into an arch-shaped line defect. (a) An isosurface of the spin magnitude is shown in green (light gray). The spin magnitude rises to 1 [dark red (black)] on the FM side of the interface ($z < 0$) and inside the Alice arch on the polar side. The singly quantized vortex with polar core remains in the FM phase. Gray cones indicate the spin vector. (b) The nematic axis (cones) retains the hedgehog structure centered on the Alice arch (the deformed point defect), indicating that the topological charge is preserved. (c) Constant-density surfaces for $n|\zeta_+|^2$ [red (medium gray)] and $n|\zeta_-|^2$ [blue (dark gray)]. The Alice arch is formed by deformation of the vortex cores in the $\zeta_\pm$ spinor components. The vortex line in ζ_+ splits at the interface (indicated by the dotted line). The upper part forms the Alice arch together with the vortex line in ζ_- above the interface. The arch (above the interface) and the spin vortex (below the interface) are indicated by silver and gold (light gray) spin isosurfaces at $|\langle\hat{\mathbf{F}}\rangle| = 0.9$ and $|\langle\hat{\mathbf{F}}\rangle| = 0.5$, respectively. ($c_0 = 2.0 \times 10^4 \hbar\omega l^3$, $|c_2| = 5.0 \times 10^2 \hbar\omega l^3$, $\Omega = 0$, and $B = 0$.)

quantized vortex in the polar part is deformed into two half-quantum vortices.

The size of a singular defect core with vanishing density is determined by $\xi_n = (8\pi c_0 n)^{-1/2}$, the density healing length. The singular polar vortex lowers its energy by spontaneously breaking axial symmetry, splitting into half-quantum vortices with FM cores of size ξ_F. The deformation is energetically favorable when the energy cost of the FM cores is smaller than the energy gained by removing the density depletion. We find the same splitting of the polar vortex for the defect with a singular vortex in both phases.

A very intriguing core deformation results from minimizing the energy of a singular spin vortex terminating on a polar monopole [Fig. 1(c)]. The point defect requires the density to go to zero. For sufficiently large ξ_F, the energy cost of the density depletion can be avoided by deforming the point defect into a semicircular line defect with FM core whose ends attach to the interface. Figure 3 shows the resulting arch-like defect.

The arch is formed as a local deformation of the point defect and retains its topological charge. Specifically, the radial hedgehog in the nematic axis $\hat{\mathbf{d}}$ is preserved away from the arch. Single-valuedness of Ψ then requires that $\hat{\mathbf{d}}$ turn by π on any closed loop through the arch, accompanied by a π change in the phase ϕ. We thus identify the line defect as an arch-shaped half-quantum vortex, which we will call an Alice arch, as it is the interface analogue of the complete Alice ring [30]. Such ring-shaped defects are analogous to Alice rings in high energy physics [42] with a topological charge similar to the magnetic ''Cheshire'' charge [43]. We find that the deformation of a point defect to an arch is energetically favorable for $c_2 \lesssim 0.5c_0$. It is unstable towards drifting out of the cloud due to the density gradient, but could be stabilized by a weak pinning potential.

Different defect structures penetrating the interface can be prepared experimentally by recognizing that the defects are composed of simple vortex lines, phase kink planes, or in more complex cases, vortex rings in the three spinor components, each of which may be phase-imprinted using existing technologies [44–46]. Vortices may also nucleate due to rotation. We find that nucleation energetically favors defects consisting of a half-quantum vortex connecting to a coreless vortex, leading to states such as that illustrated in Fig. 1(g).

Here we have demonstrated topological interface engineering by studying examples of defect perforation across a FM-polar interface in a spin-1 BEC. Vortex bifurcation purely due to an energetic (not topological) effect in the phase separation of a two-species BEC was studied in Refs. [47,48]. Our method can be extended to more complex broken symmetries in spin-2 [25,26,31] and spin-3 [27,28] BECs that also support, e.g., non-Abelian defects [32,49]. Other particularly promising systems for topological interface physics are strongly correlated atoms in optical lattices [15–17] exhibiting also quantum phase transitions and potential analogues of exotic superconductivity [1] in crystal lattices.

Nonequilibrium defect production may be investigated in phase transitions in the presence of different broken symmetries [5,9]. Defect formation from colliding interfaces can be employed as a model to simulate cosmological brane annihilation [7,8]. For instance, in a FM condensate, a slab of polar phase could be created, each interface being a 2D analogue of a D-brane. Removing the interaction shift causes the slab to collapse, bringing the interfaces closer until they meet and annihilate,

representing an annihilation of a brane-antibrane pair. In braneworld scenarios of cosmic inflation the annihilation may lead to defect production [7] that could be directly observed in atomic BECs. A similar experiment has been performed with superfluid liquid ^{3}He A-B interfaces in which case, however, the detection of defects is difficult [10].

We acknowledge discussions with D. J. Papoular and M. D. Lee and financial support from Leverhulme Trust.

*M.O.Borgh@soton.ac.uk
†janne@soton.ac.uk

[1] J. A. Bert, B. Kalisky, C. Bell, M. Kim, Y. Hikita, H. Y. Hwang, and K. A. Moler, Nature Phys. **7**, 767 (2011).
[2] M. M. Salomaa, Nature (London) **326**, 367 (1987).
[3] G. E. Volovik, *The Universe in a Helium Droplet* (Oxford University Press, Oxford, 2003).
[4] A. P. Finne, V. B. Eltsov, R. Hänninen, N. B. Kopnin, J. Kopu, M. Krusius, M. Tsubota, and G. E. Volovik, Rep. Prog. Phys. **69**, 3157 (2006).
[5] T. W. B. Kibble, J. Phys. A **9**, 1387 (1976).
[6] A. Vilenkin and E. P. S. Shellard, *Cosmic Strings and Other Topological Defects* (Cambridge University Press, Cambridge, 1994).
[7] S. Sarangi and S.-H. H. Tye, Phys. Lett. B **536**, 185 (2002).
[8] G. Dvali and S.-H. H. Tye, Phys. Lett. B **450**, 72 (1999).
[9] W. H. Zurek, Nature (London) **317**, 505 (1985).
[10] D. I. Bradley, S. N. Fisher, A. M. Guenault, R. P. Haley, J. Kopu, H. Martin, G. R. Pickett, J. E. Roberts, and V. Tsepelin, Nature Phys. **4**, 46 (2008).
[11] E. B. Bogomolny, Sov. J. Nucl. Phys. **24**, 449 (1976).
[12] R. Jackiw and C. Rebbi, Phys. Rev. D **13**, 3398 (1976).
[13] N. Manton and P. Sutcliffe, *Topological Solitons* (Cambridge University Press, Cambridge, 2004).
[14] L. Faddeev and A. J. Niemi, Nature (London) **387**, 58 (1997).
[15] M. Greiner, O. Mandel, T. Esslinger, T. W. Hänsch, and I. Bloch, Nature (London) **415**, 39 (2002).
[16] R. Jördens, N. Strohmaier, K. Günter, H. Moritz, and T. Esslinger, Nature (London) **455**, 204 (2008).
[17] U. Schneider, L. Hackermüller, S. Will, T. Best, I. Bloch, T. A. Costi, R. W. Helmes, D. Rasch, and A. Rosch, Science **322**, 1520 (2008).
[18] C. N. Weiler, T. W. Neely, D. R. Scherer, A. S. Bradley, M. J. Davis, and B. P. Anderson, Nature (London) **455**, 948 (2008).
[19] L. E. Sadler, J. M. Higbie, S. R. Leslie, M. Vengalattore, and D. M. Stamper-Kurn, Nature (London) **443**, 312 (2006).
[20] Y. Lin, R. L. Compton, K. Jimenez-Garcia, J. V. Porto, and I. B. Spielman, Nature (London) **462**, 628 (2009).
[21] J. Stenger, S. Inouye, D. M. Stamper-Kurn, H. Miesner, A. P. Chikkatur, and W. Ketterle, Nature (London) **396**, 345 (1998).
[22] T.-L. Ho, Phys. Rev. Lett. **81**, 742 (1998).
[23] T. Ohmi and K. Machida, J. Phys. Soc. Jpn. **67**, 1822 (1998).
[24] F. Zhou, Int. J. Mod. Phys. B **17**, 2643 (2003).
[25] M. Koashi and M. Ueda, Phys. Rev. Lett. **84**, 1066 (2000).
[26] C. V. Ciobanu, S.-K. Yip, and T.-L. Ho, Phys. Rev. A **61**, 033607 (2000).
[27] R. Barnett, A. Turner, and E. Demler, Phys. Rev. Lett. **97**, 180412 (2006).
[28] L. Santos and T. Pfau, Phys. Rev. Lett. **96**, 190404 (2006).
[29] H. T. C. Stoof, E. Vliegen, and U. Al Khawaja, Phys. Rev. Lett. **87**, 120407 (2001).
[30] J. Ruostekoski and J. R. Anglin, Phys. Rev. Lett. **91**, 190402 (2003).
[31] G. W. Semenoff and F. Zhou, Phys. Rev. Lett. **98**, 100401 (2007).
[32] M. Kobayashi, Y. Kawaguchi, M. Nitta, and M. Ueda, Phys. Rev. Lett. **103**, 115301 (2009).
[33] M. Vengalattore, S. R. Leslie, J. Guzman, and D. M. Stamper-Kurn, Phys. Rev. Lett. **100**, 170403 (2008).
[34] J. Kronjäger, C. Becker, P. Soltan-Panahi, K. Bongs, and K. Sengstock, Phys. Rev. Lett. **105**, 090402 (2010).
[35] A. E. Leanhardt, Y. Shin, D. Kielpinski, D. E. Pritchard, and W. Ketterle, Phys. Rev. Lett. **90**, 140403 (2003).
[36] L. S. Leslie, A. Hansen, K. C. Wright, B. M. Deutsch, and N. P. Bigelow, Phys. Rev. Lett. **103**, 250401 (2009).
[37] See Supplemental Material at http://link.aps.org/supplemental/10.1103/PhysRevLett.109.015302 for basic defect configurations in spin-1 BECs and the construction of prototype spinor wave functions for vortex connections across the interface.
[38] F. K. Fatemi, K. M. Jones, and P. D. Lett, Phys. Rev. Lett. **85**, 4462 (2000).
[39] D. J. Papoular, G. V. Shlyapnikov, and J. Dalibard, Phys. Rev. A **81**, 041603 (2010).
[40] C. M. Savage and J. Ruostekoski, Phys. Rev. A **68**, 043604 (2003).
[41] The results are qualitatively similar in the presence of a weak Zeeman splitting ($|g_1\mathbf{B}| \leq 10^{-1}\hbar\omega$) to the case of $\mathbf{B} = 0$. We also checked that fixing the magnetization $M = N_+ - N_-$. (where $N_\pm$ are the total populations of $\zeta_\pm$) during the relaxation does not alter the basic results.
[42] A. S. Schwarz, Nucl. Phys. **B208**, 141 (1982).
[43] M. Alford, K. Benson, S. Coleman, J. Marchrussel, and F. Wilczek, Nucl. Phys. **B349**, 414 (1991).
[44] M. R. Matthews, B. P. Anderson, P. C. Haljan, D. S. Hall, C. E. Wieman, and E. A. Cornell, Phys. Rev. Lett. **83**, 2498 (1999).
[45] J. Ruostekoski and J. R. Anglin, Phys. Rev. Lett. **86**, 3934 (2001).
[46] J. Ruostekoski and Z. Dutton, Phys. Rev. A **72**, 063626 (2005).
[47] H. Takeuchi and M. Tsubota, J. Phys. Soc. Jpn. **75**, 063601 (2006).
[48] K. Kasamatsu, H. Takeuchi, M. Nitta, and M. Tsubota, J. High Energy Phys. 011 (2010) 068.
[49] J. A. M. Huhtamäki, T. P. Simula, M. Kobayashi, and K. Machida, Phys. Rev. A **80**, 051601 (2009).